Materials Research Bulletin 49 (2014) 618–624

Contents lists available at ScienceDirect

Materials Research Bulletin

journal homepage: www.elsevier.com/locate/matresbu

Visible light absorption of TiO_2 materials impregnated with tungstophosphoric acid ethanol–aqueous solution at different pH values. Evidence about the formation of a surface complex between Keggin anion and TiO_2 surfaces

Julián A. Rengifo-Herrera *, Mirta N. Blanco, Luis R. Pizzio *

Centro de Investigación y Desarrollo en Ciencias Aplicadas "Dr. J.J. Ronco" (CINDECA), Departamento de Química, Facultad de Ciencias Exactas, UNLP-CCT La Plata, CONICET, 47 No. 257, 1900 La Plata, Buenos Aires, Argentina

ARTICLE INFO

Article history:
Received 20 March 2013
Received in revised form 3 September 2013
Accepted 29 September 2013
Available online 8 October 2013

Keywords:
A. Composites
A. Nanostructures
A. Semiconductors
D. Optical properties
C. Raman spectroscopy

ABSTRACT

TiO_2 particles prepared by the sol–gel method were impregnated at different pH values (1.0, 2.0, 5.0 and 10.0) with a water–ethanol solution (50% V/V) of tungstophosphoric acid (TPA) (0.012 M). Similar preparation was carried out to synthesize TiO_2 impregnated with $[WO_4]^{2-}$ (TiW). These materials were characterized by different techniques such as UV–vis diffuse reflectance spectroscopy (UV–vis DRS), magic angle spinning nuclear magnetic resonance of ^{31}P (^{31}P MAS NMR), X-ray diffraction (XRD), Fourier transform infrared spectroscopy (FT-IR), Fourier transform Raman spectroscopy (FT-Raman).

Results revealed that TPA–TiO_2 materials exhibit visible light absorption only when impregnation was done at pH 1.0 (TiTPA1) and 2.0 (TiTPA2). TiW powder did not show visible light absorption. XRD patterns show the presence of peaks at $2\theta = 25.4^\circ$ (1 0 1), 37.9° (0 0 4), 47.8° (2 0 0) and 54.3° associated to the anatase phase. Solid NMR, FT-IR and FT-Raman characterization showed that TiTPA1 and TiTPA2 samples contain Keggin ($[PW_{12}O_{40}]^{3-}$) and lacunary anions ($[PW_{11}O_{39}]^{7-}$) respectively. On the other hand, FT-Raman results revealed a blue shifting and broadening of the band at 141 cm^{-1} corresponding to anatase TiO_2 and moreover, a broadening of bands at 900–1100 cm^{-1} attributed to Keggin structures of TPA. Both spectral changes could be related to the formation of a surface complex between the Keggin anion of TPA and TiO_2 surfaces. This interaction should be responsible for visible light absorption.

1. Introduction

Heterogeneous photocatalysis on TiO_2 has risen as a promising technology to destroy and inactivate waterborne pollutants and microorganisms [1–3]. However, nowadays the future outlooks in heterogeneous photocatalysis are addressed to the preparation of novel TiO_2 photocatalysts that show visible light absorption (more abundant on the terrestrial surface) and low electron/hole recombination [4,5].

Different strategies have been proposed in the literature to achieve these goals. Regarding the preparation of TiO_2 materials with visible light absorption, the two most explored strategies have been the doping with metallic (i.e. Cr, V and Fe) [6] and nonmetallic (i.e. N and S) elements [7]. Although both procedures yield visible light absorption on TiO_2, their photocatalytic activities under UV or visible light absorption are still under debate since some studies have revealed that the presence of metals on TiO_2 surfaces could induce recombination centers increasing electron–hole (e^-/h^+) recombination and producing a detrimental effect on the photocatalytic activity [8]. On the other hand, doping with N or S might induce the creation of mid-gap levels in TiO_2, which could produce the photogeneration of holes with lower oxidant potential avoiding the generation of higher oxidant •OH radicals and decreasing its photocatalytic activity [9,10].

Regarding e^-/h^+ recombination on TiO_2 particles, it has been successfully decreased by the addition of noble metals on the oxide surface [11]. Metals such as silver, platinum and gold behave as acceptors of photoinduced electrons allowing a better charge separation [11,12]. However, recently it has been proposed that Ag–TiO_2 materials can undergo silver dissolution by the presence of H_2O_2 and UV light, thus leaching Ag^+ ions to the solution [13]. Heteropolyoxometallates (POMs) are clusters of transition metals and oxygen that are widely used as oxidation as well as acid catalysts [14–16]. POMs have often been used as effective

* Corresponding authors at: CINDECA, Calle 47 No. 257, 1900 La Plata, Argentina. Tel.: +54 221 421 1353; fax: +54 221 421 1353x125.
E-mail addresses: julianregifo@quimica.unlp.edu.ar (J.A. Rengifo-Herrera), lrpizzio@quimica.unlp.edu.ar (L.R. Pizzio).

0025-5408/$ – see front matter © 2013 Elsevier Ltd. All rights reserved.
http://dx.doi.org/10.1016/j.materresbull.2013.09.043

homogeneous photocatalysts in the oxidation of organic compounds [14] and in the degradation of organic pollutants in water [17].

The incorporation of POMs such as tungstophosphoric acid (TPA) on TiO_2 has been explored as an alternative route to decrease the e^-/h^+ recombination and to enlarge light absorption ability. It is well known that the incorporation of TPA on a TiO_2 surface enhances its photocatalytic activity since POM can act as an efficient electron acceptor [18–20]. On the other hand, different studies have reported that the addition of TPA on TiO_2 particles can lead to visible light absorption [21–25]. However, this latter issue has not been well stated. Different proposals have been suggested in the literature. For instance, some authors have argued that the visible light absorption of TiO_2–TPA materials is probably due to phosphorous doping (P-doping), since during the material preparation, TPA can undergo total or partial degradation leading to phosphate (PO_4^{3-}) and WO_3 formation [22]. The former would be responsible for its visible light absorption and the latter for its lower e^-/h^+ recombination. Recently, Lu et al. [25] have oriented the discussion towards the formation of TiO_2–Keggin–TPA composites; this might lead to generation of a mid-gap level close to the TiO_2 conduction band (CB) and be responsible for its visible light absorption.

Herein, different TiO_2-based materials were prepared by incorporation of TPA (0.012 M) to a solution composed of ethanol–water (50% V/V) and TiO_2 xerogel under different initial pH values. Furthermore TiO_2 was impregnated with WO_4^{2-} to compare the physical–chemical features. These materials were characterized by different techniques such as: UV–vis-DRS, ^{31}P MAS NMR, FT-IR, XRD and FT-Raman spectroscopy. Results suggest the existence of a complex formation between the Keggin or lacunar TPA anions and TiO_2 and this complex should be responsible for the visible light absorption of these materials.

2. Experimental

2.1. Synthesis of TPA–TiO_2 particles

Titanium isopropoxide (Aldrich, 16 mL) was mixed with absolute ethanol (Merck, 60 mL) and stirred for 10 min to obtain a homogeneous solution under N_2 at room temperature, then 90 μL of concentrate aqueous ammonia was dropped slowly into the above mixture to catalyze the sol–gel reaction and was left for 1 h at 80 °C. Ammonium excess was eliminated from the gel by washing several times until the pH of the washing effluent was neutral. Then an amount of $H_3PW_{12}O_{40}{\cdot}23H_2O$ (Fluka p.a.) was dissolved in 50 mL of a solution of 50% ethanol–water to reach a TPA concentration of 0.012 M and at different initial pH values (1.0, 2.0, 5.0 and 10.0) (adjusted by adding NaOH or HCl). The prepared gel (7.2 g) was added to these solutions in order to obtain a TPA/TiO_2 ratio (30% (w/w), equivalent to 22.9% (w/w) of W in the final material) and was left until complete drying of the solvent. The dry gel was washed three times to remove weakly bonded TPA or related species. Finally, the gel was annealed at 500 °C for 1 h. Hereinafter, the samples will be referred as TiTPAX, where *X* indicates the initial pH of the TPA solution used to prepare them.

The sample containing tungstate anions (TiW) was obtained following the previous procedure but adding a 0.144 M Na_2WO_4 (Sigma–Aldrich p.a.) aqueous solution instead of $H_3PW_{12}O_{40}{\cdot}23H_2O$.

The W content on the TiTPAX and TiW samples was estimated as the difference between the W amount contained in the TPA (and Na_2WO_4) solutions and the remaining amount of W in the beaker after the impregnation of TiO_2. The amount of W remaining after the impregnation of TiO_2 in the beaker was determined by atomic absorption spectrometry using a Varian AA Model 240 spectrophotometer. The calibration curve method was used with standards prepared in the laboratory. The analyses were carried out at a wavelength of 254.9 nm, bandwidth 0.3 nm, lamp current 15 mA, phototube amplification 800 V, burner height 4 mm, and acetylene–nitrous oxide flame (11:14). The results obtained revel that the W content in the samples were 22.5; 21.9, 22.3; 23.2 and 22.6% (w/w) for the TiTPA1, TPA2, TPA5, TPA10 and TiW samples, respectively.

2.2. Sample characterization

2.2.1. Diffuse reflectance spectroscopy (DRS)

The diffuse reflectance spectra of the materials were recorded using a UV–visible Lambda 35, Perkin Elmer spectrophotometer, to which a diffuse reflectance chamber Labsphere RSA-PE-20 with an integrating sphere of 50 mm diameter and internal Spectralon coating is attached, in the 250–800 nm wavelength range. Spectralon was used as reference.

2.2.2. X-ray diffraction (XRD) measurements

X-ray diffraction patterns of samples were recorded using Phillips PW 1732 equipment with built-in recorder and CuKα radiation, nickel filter, 20 mA and 40 kV in the high voltage source, and scanning angle between 5 and 60° of 2θ at a scanning rate of $1^\circ\ min^{-1}$.

2.2.3. Nuclear magnetic resonance spectroscopy (NMR)

The ^{31}P magic angle spinning-nuclear magnetic resonance (^{31}P MAS NMR) spectra were recorded with Bruker Avance II equipment, using the CP/MAS ^1H–^{31}P technique. A sample holder of 4 mm diameter and 10 mm in height was employed, using 5 ms pulses, a repetition time of 4 s, and working at a frequency of 121.496 MHz for ^{31}P at room temperature. The spin rate was 8 kHz and several hundred pulse responses were collected. Phosphoric acid 85% was employed as external reference.

2.2.4. Fourier transform infrared spectroscopy (FT-IR)

FT-IR spectra of the supports and catalysts were obtained in the 400–4000 cm^{-1} wavenumber range using Bruker IFS 66 FT-IR spectrometer and pellets in KBr.

2.2.5. Fourier transform Raman spectroscopy (FT-Raman)

Raman scattering spectra were recorded on a Raman Horiba Jobin-Yvon T 64000 instrument with an Ar^+ laser source of 488 nm wavelength in a macroscopic configuration.

3. Results

3.1. UV–vis DRS characterization

Fig. 1 shows the DRS spectra recorded on the TPA and $[WO_4]^{2-}$ impregnated samples, pristine TiO_2 and bulk TPA. Bulk TPA exhibits two intense absorption bands at 200 and 260 nm corresponding to $O_d \rightarrow M$ and $O_b/O_c \rightarrow M$, respectively [16,26]. In the case of bulk Na_2WO_4 only an absorption band at 220 nm assigned to the $O_d \rightarrow M$ charge transfer was detected [27]. On the other hand, TiO_2 shows an intense band absorption at $\lambda < 400$ nm, attributed to transitions from the valence band to the conduction band [28]. All TPA–TiO_2 materials impregnated at different pH values (TiTPA1, TiTPA2, TiTPA5, TiTPA10 samples) exhibited UV light absorption ($\lambda < 400$) due to the presence of TPA and TiO_2. However, it was not possible to identify the characteristic single absorption bands corresponding to TPA and TiO_2. The TPA–TiO_2 materials obtained by impregnation at pH 1 and 2 (TiTPA1 and TiTPA2 samples) showed, in addition, visible light absorption at wavelengths between 400 and 450 nm, whereas powders impregnated at higher pH values (TiTPA5 and TiTPA10 samples) and

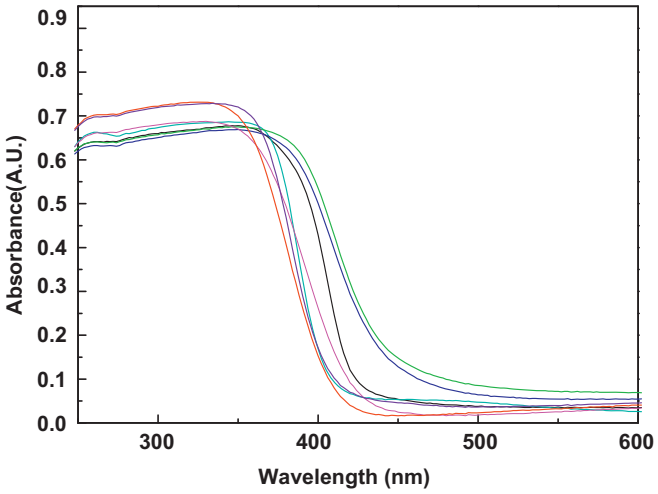

Fig. 1. DR spectrum of synthesized powders. (▬) TITPA1, (▬) TITPA2, (▬) TITPA5, (▬) TITPA10, (▬) TiO_2, (▬) TiW, and (▬) TPA.

impregnated with $[WO_4]^{2-}$ (TiW) ethanol–aqueous solutions did not exhibit visible light absorption.

3.2. X-ray diffraction characterization

Fig. 2 shows the XRD patterns of TiO_2 samples impregnated with TPA. XRD patterns show the presence of peaks at $2\theta = 25.4^\circ$ (1 0 1), 37.9° (0 0 4), 47.8° (2 0 0) and 54.3° related with TiO_2 anatase phase. In addition, no diffraction lines attributed to crystalline TPA were observed, indicating that TPA has been highly dispersed in the titania matrix as it was previously reported [29].

3.3. FT-Raman and FT-IR characterization

FT-Raman spectra of pristine TiO_2, bulk TPA, TiO_2–TPA samples and TiO_2-$[WO_4]^{2-}$ were recorded and are shown in Fig. 3a. Anatase TiO_2 belongs to the tetragonal space group D_{4h}^{1g} ($I4_1/amd$), which exhibits six Raman active modes ($A_{1g}+2B_{1g}+3E_g$): at 141.3 cm^{-1} (E_g), 394.4 cm^{-1} (B_{1g}), 516.1 cm^{-1}, (A_{1g}, B_{1g}) and 636.7 cm^{-1} (E_g) [30,31]. Fig. 3a shows the Raman spectrum of pristine TiO_2 revealing four bands at 141, 393, 515 and 636 cm^{-1} that agree very well with anatase TiO_2 phase. On the other hand, the FT-Raman spectrum of bulk TPA showed Raman vibration bands typically assigned to Keggin anion at 1080, 990, 930, and 890 cm^{-1}, which

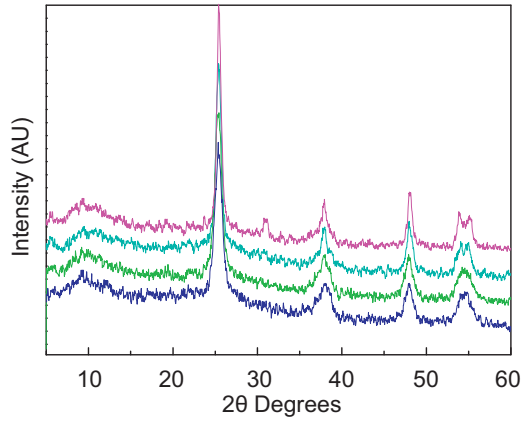

Fig. 2. FT-IR spectrum of TiO_2 samples impregnated with TPA. (▬) TITPA1, (▬) TITPA2, (▬) TITPA5, (▬) TITPA10, and (▬) TPA.

are attributed to antisymmetric vibrations of P–O, W=O and W–O–W bonds [32,33].

TiTPA1, TiTPA2, and TiTPA5 materials exhibited Raman vibrations of anatase TiO_2 and a broad band between 970 and 1020 cm^{-1} (Fig. 3c). The latter has already been assigned to the presence of TPA in TiO_2 materials [34]. Regarding the material TiTPA10, it did not show any signal in the 970–1020 cm^{-1} region. On the other hand, the Raman spectrum of TiW powder (Fig. 3a) showed only the same four bands assigned to anatase TiO_2.

Fig. 3b shows a zoom done on the most intense band at 141 cm^{-1} that is often assigned to anatase TiO_2 [35]. This signal underwent a strong blue shifting (shifting to higher wavenumber), an intensity decrease and a band broadening in the samples TiTPA1, TiTPA2, TiTPA5 and TiTPA10. This shifting was more intense (around 10 cm^{-1}) in TiTPA1 material. In the TiW sample, these characteristics were not observed. The blue shifting could be related to phonon confinement and particle size reduction [31]. However, some authors have claimed that shifting and broadening of the Raman band at 141 cm^{-1} in anatase TiO_2 could also be due to deviations from stoichiometry [30,35]. This Raman band arises from O–Ti–O band-bending-type vibrations; thus this shifting may be related to the presence of oxygen deficiencies or disorders induced by minority phases [30,35–37]. Moreover, Li et al. [33] have argued that shifting and broadening of Raman vibration modes on TPA and TiO_2 could also be associated with a strong interaction between the TiO_2 network and TPA.

The FT-IR spectra of TiO_2 impregnated with TPA and bulk TPA are shown in Fig. 4. Tungstophosphoric acid exhibits IR bands at 1080, 982, and 892 cm^{-1} ascribed to ν_{as} (P–O), ν_{as} (W–O) and ν_{as} (W–O–W) vibrations, respectively, attributed to Keggin anion [27,32,38]. The pristine TiO_2 and TiW sample showed IR bands at 700 cm^{-1} ascribed to Ti–O–Ti stretching vibration (data not shown).

The samples TiTPA1, TiTPA2, and TiTPA5 showed IR bands corresponding to the Keggin anion at 1076 and 976 cm^{-1}, whereas the sample TiTPA10 exhibited IR bands at 1100, 1048, 935 and 883 cm^{-1}. At high pH values, the Keggin anion of TPA undergoes depolymerisation towards the formation of monovacant $[PW_{11}O_{39}]^{7-}$ (at pH >5) and trivacant lacunary anions $[PW_9O_{34}]^{9-}$ (at pH >8) [27,32].

The sample TiTPA10 shows some bands related to the presence of the lacunary anions or products of their fragmentation. Results show that all IR vibration bands corresponding to TPA underwent red shifting possibly due to TiO_2–TPA interactions.

3.4. Characterization by ^{31}P MAS NMR

Fig. 5 shows the spectra recorded by ^{31}P MAS NMR. The spectrum of the sample TiTPA1 exhibits two peaks with a chemical shift at −14.6 (very intense) and −13.2 (low intensity) ppm, attributed to Keggin anion and the dimeric $[P_2W_{21}O_{71}]^{6-}$ anion, respectively [27,32]. TiTPA2 also showed both the intense peak assigned to $[PW_{12}O_{40}]^{3-}$ anion and the weak peak corresponding to $[P_2W_{21}O_{71}]^{6-}$ anion. On the other hand, sample TiTPA5 exhibited only a weak peak at −14.6 ppm corresponding to the Keggin anion.

The sample TiTPA10 did not show evidence about the presence of Keggin or dimeric anions. An intense peak at 3.3 ppm corresponding to PO_4^{3-} species was found [32].

4. Discussion

Characterization results suggest that impregnation of TPA on TiO_2 at low pH (1 and 2) leads mainly to the presence of Keggin anion on TiO_2 surfaces. With increasing pH, the Keggin anion partially decomposes to give dimeric and lacunary anions [27,32].

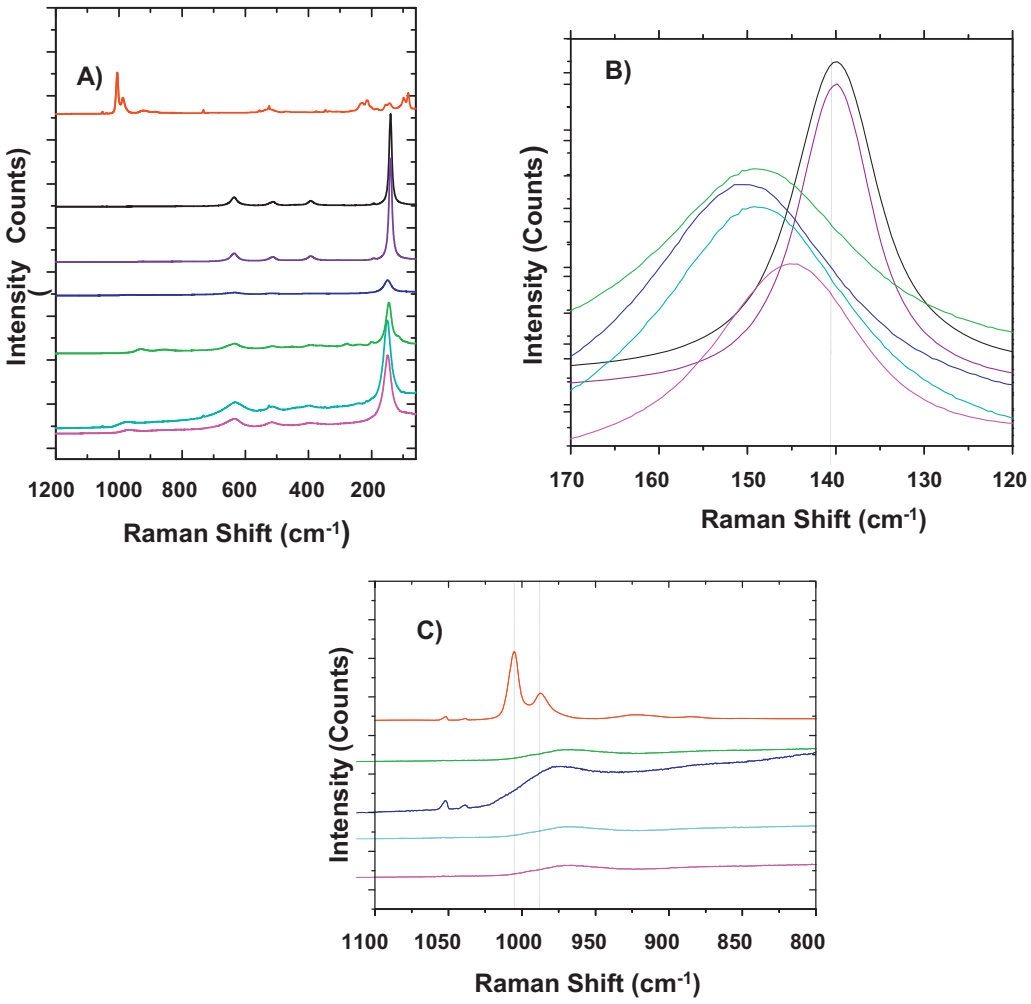

Fig. 3. XRD patterns of samples impregnated with TPA. (—) TITPA1, (—) TITPA2, (—) TITPA5, and (—) TITPA10.

It is well known that at pH 1.5–2.0, the Keggin anion is reversibly and quickly transformed into the lacunar species $[PW_{11}O_{39}]^{7-}$. Pope [38] has proposed that the following transformation scheme: $[PW_{12}O_{40}]^{3-} \Leftrightarrow [P_2W_{21}O_{71}]^{6-} \Leftrightarrow [PW_{11}O_{39}]^{7-}$ takes place when the pH is increased. This transformation is due to the limited stability range of the $[PW_{12}O_{40}]^{3-}$ anion in solution, which can be increased by adding an organic solvent such as ethanol [38]. The main FT-IR bands of the dimer $[P_2W_{21}O_{71}]^{6-}$ assigned to the stretching vibrations P–O, W–O, W–O–W appear at wavenumber values similar to those characteristic of the $[PW_{12}O_{40}]^{3-}$ anion [40]. Taking into account this fact and ^{31}P MAS NMR results, we can assume that the FT-IR bands at 890 and 790 cm^{-1} are due to the presence of both $[PW_{12}O_{40}]^{3-}$ and $[P_2W_{21}O_{71}]^{6-}$ species.

Although in the literature it is suggested that the Keggin anion of tungstophosphoric acid is only stable at pH < 2.0, recently Holclajtner-Antunovic et al. [32] have demonstrated that these species can be stable at pH values between 2 and 5 in aqueous/methanol mixtures. This is because methanol and others alcohols such as ethanol, protects the Keggin anion from hydrolysis, which can decompose it. Moreover, our results show that visible light absorbing TiO_2 is only produced when the Keggin structure is mainly present on the TiO_2 surface (TiTPA1 and TiTPA2 samples). On the other hand, FT-Raman and FT-IR characterization revealed shifting of some bands with respect to TPA and TiO_2. All these results suggest the existence of a strong interaction between Keggin anion and TiO_2 surfaces leading to the formation of a visible light absorption complex. Different studies have reported that the formation of a charge-transfer complex between TiO_2 and adsorbates (such as catechol and EDTA) can take place, leading to visible light absorption [37]. Moreover, polyoxometallates such as tungstophosphoric acid can act as ligand by binding metal cations via surface terminal and bridging oxygen atoms and defects (lacunary structures) enclosing cations in the vacancies [34]. Li et al. [34] have argued that interactions between TiO_2 and TPA can take place through H-bonding between O atoms of the Keggin anion and the surface Ti–OH groups of TiO_2 network. Yang et al. have suggested that ionic pairs ($\equiv TiOH_2^+$–TPA^-) could be responsible of TPA–TiO_2 interactions [23]. Fuchs et al. [29] have also argued that these ionic pairs are produced due to transfer of tungstophosphoric acid protons to Ti–OH according to:

$$Ti{-}OH + H_3PW_{12}O_{40} \rightarrow [Ti{-}OH_2^+][H_2PW_{12}O_{40}^-] \quad (1)$$

We suggest that when TPA is added to TiO_2 colloids, an interaction could take place, which is produced by hydrogen bonding of $W{-}O_t \ldots HO{-}Ti$ bonds. Moreover, during material annealing, the formation of oxygen vacancies (coordinatively unsaturated (Ti^{IV}) species) could occur and these Ti^{IV} species might interact with W–O bonds from TPA yielding strong interactions responsible for visible light absorbing complex formation. However, the mechanism reported by Li et al. [34] where the TPA–TiO_2 interactions occur only by H-bonding and formation of ionic pairs claimed by Yang et al. [23] could be also responsible of these polyoxometalate–semiconductor interactions.

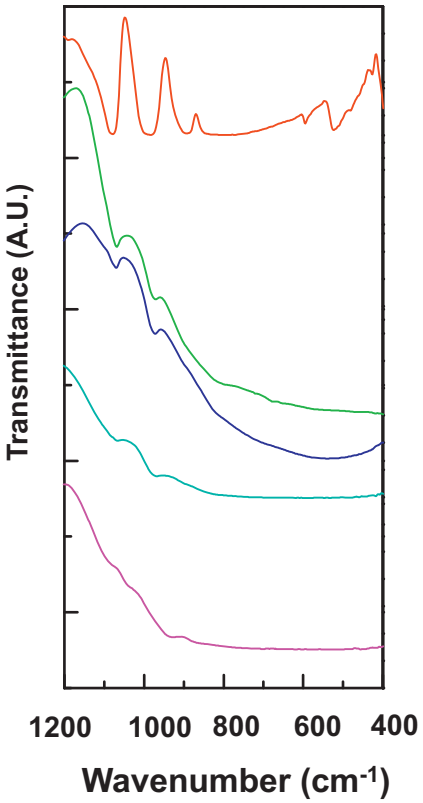

Fig. 4. FT-Raman spectra of synthesized samples. (—) TITPA1, (—) TITPA2, (—) TITPA5, (—) TITPA10, (—) TiO_2, (—) TiW, and (—) TPA.

The visible light photocatalytic activity of TPA–modified TiO_2 has not been extensively studied in the literature. Few studies reporting the visible light absorption of TiO_2 materials modified with tungstophosphoric acid have been found. For instance, Lu et al. [25] have argued that TiO_2–TPA materials prepared by the sol–gel method absorb visible light by the fact that a new conduction band (CB) might be constructed from the hybridization of Ti 3d and W 5d orbitals. On the other hand, Yu et al. [22] report that tungstophosphoric acid is completely decomposed by annealing at 350 °C of gels prepared by acid hydrolysis of titanium tetraisopropoxide and impregnated with TPA. This thermal decomposition of TPA leads to the formation of WO_3 and P-doping of TiO_2; the latter would be responsible for its visible light absorption. Recently, we have proposed [21] that visible light absorption of TiO_2 materials prepared by sol–gel and modified with TPA was due to the presence of WO_x species, such as WO_3 coming from the partial degradation of TPA. However, our results from the present study show that TPA is stable even under annealing at 500 °C as it was observed by ^{31}P NMR measurements.

All the TiO_2 materials prepared with TPA reported in the literature always show high photocatalytic activity under visible light irradiation. However, the study reported by Lu et al. [25] is not clear about the exact position of the new CB created by the TPA on TiO_2. This position is a key point since the CB must have a high enough redox potential to reduce molecular oxygen, thus avoiding the e^-/h^+ recombination.

Herein it is reported that the Keggin anion undergoes a strong interaction with TiO_2 surfaces yielding a surface complex between TiO_2 and TPA Keggin anion responsible for its visible light absorption. TPA complexed on TiO_2 surfaces could retain the same physicochemical features as that of bulk TPA. Thus, the photocatalytic activity of these materials under UV and visible light irradiation can be explained.

Under UV light irradiation, TPA behaves as an excellent photoelectron sink, decreasing e^-/h^+ recombination [19,39,41,42]. This leads to TiO_2 materials with a higher photocatalytic activity since it is well known that the first potential reduction of TPA is more positive than the redox potential of the photoexcited electron on the conduction band [16] (Fig. 6). Thus the photoexcited electron can easily be transferred to the TPA complex on the TiO_2 surface.

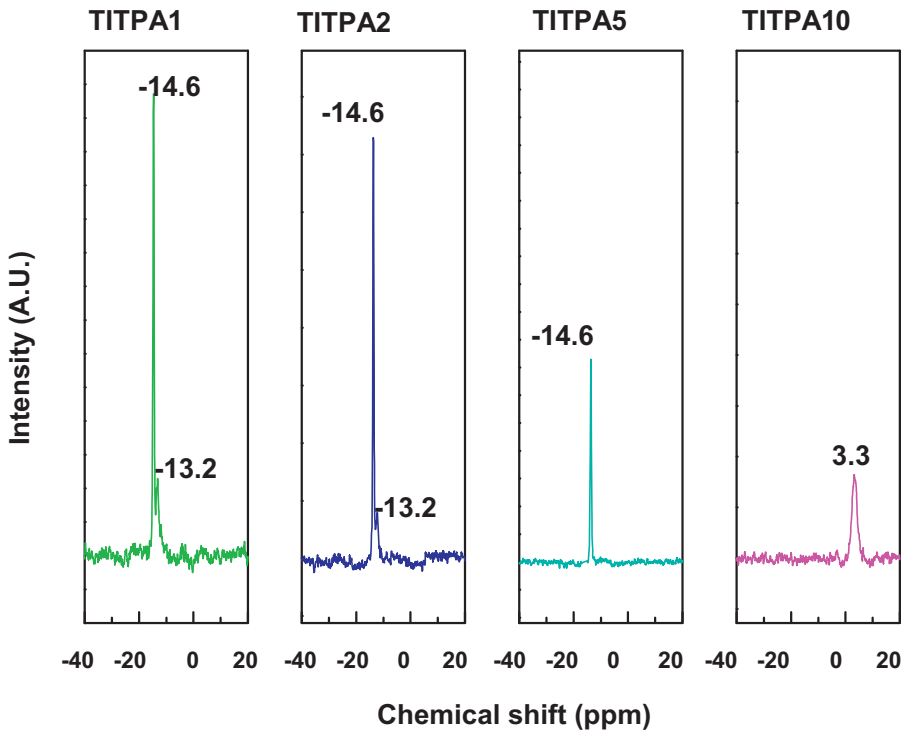

Fig. 5. ^{31} P MAS NMR spectra of TiO_2 powders impregnated with TPA.

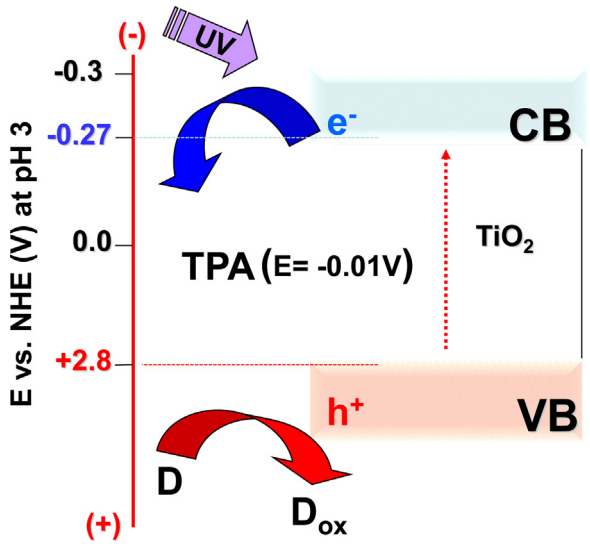

Fig. 6. Scheme suggested for the photocatalytic process occurring in TiO_2–TPA systems upon UV-light irradiation.

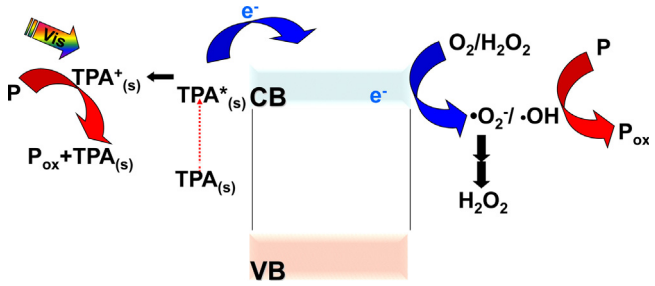

Fig. 7. Proposed scheme of the photocatalytic process occurring in TiO_2–TPA systems upon vis-light irradiation.

On the other hand, under visible light irradiation the mechanism could be more complex (Fig. 7). Upon this irradiation, TPA anchored to the TiO_2 surface (TPA–TiO_2) would be excited yielding TPA*–TiO_2. It is well known that the excited states of polyoxometallates are excellent electron donors and acceptors since they have a lower ionization energy and increased electron affinity [16], thus the TPA*–TiO_2 excited state complex can inject a photoexcited electron to the TiO_2 CB yielding oxidized TPA^+–TiO_2 species; the latter species can accept an electron from an organic pollutant previously adsorbed on the TiO_2 surface regenerating the TPA–TiO_2 complex and oxidizing the pollutant. Some studies in the literature have suggested that the electron transfer from TPA* to TiO_2 CB could take place in the presence of polyvinyl alcohol [43]. Furthermore, Tachikawa et al. [44] have proposed, by using flash photolysis techniques, that one electron oxidation of aromatic sulfides takes place through a mechanism involving electron transfer from TPA* to TiO_2 CB.

On the other hand, electron injected to TiO_2 CB can react with molecular oxygen yielding a superoxide radical. It is well known that in aqueous media this radical can undergo disproportion reactions producing mainly H_2O_2 [45]. Peroxide hydrogen can be also reduced by CB electrons producing •OH radicals that are also able to oxidize organic pollutants.

5. Conclusions

Impregnation of tungstophosphoric acid on TiO_2 nanoparticles was achieved at different pH values (1.0, 2.0, 5.0 and 10.0). Visible light absorbing TiO_2 materials were only obtained at low pH values (1.0 and 2.0) where the Keggin anion was mainly present on the TiO_2 surface. FT Raman results showed that the main Raman peak of TiO_2 at 141 cm^{-1} underwent a blue shifting possibly induced by a strong interaction between the Keggin anion and the TiO_2 surface. Moreover, FT-Raman peaks of TPA were also modified since a broad peak in the region of 900–1000 cm^{-1} was observed, also revealing the possible existence of a strong interaction between TPA and TiO_2. We suggest that visible light absorption of TiO_2 modified by TPA could be due to the formation of a complex between the Keggin anion and surface defects of TiO_2 such as Ti^{IV} and/or Ti–OH sites.

Visible light photocatalytic activity of these materials in the destruction of waterborne pollutants could be explained by the fact that this surface TPA–TiO_2 complex might be excited by visible light absorption, yielding an excited state of TPA–TiO_2 complex. This excited state might inject an electron to the TiO_2 CB leaving an oxidized TPA^+–TiO_2 complex, which could accept an electron from the organic pollutant. On the other hand, the electron injected to the TiO_2 CB could be trapped by molecular oxygen adsorbed previously on the metal oxide surface leading to the formation of H_2O_2 and finally •OH radicals.

In spite of these encouraging results further experiments are necessary to determine the real behavior and role of TPA present on TiO_2 surfaces.

Acknowledgements

Authors thank CONICET and National University of La Plata (UNLP) for their support to the projects PIP 1938 and X-603 respectively.

References

[1] A. Fujishima, X. Zhang, D.A. Tryk, Surf. Sci. Rep. 68 (2008) 515–582.
[2] S. Kwon, M. Fan, A.T. Cooper, H. Yang, Crit. Rev. Environ. Sci. Technol. 38 (2008) 197–226.
[3] O.K. Dalrymple, E. Stefanakos, M.A. Trotz, D.Y. Goswami, Appl. Catal. B: Environ. 98 (2010) 27–38.
[4] N. Serpone, A.V. Emeline, J. Phys. Chem. Lett. 3 (2012) 673–677.
[5] D. Mitoraj, H. Kisch, Solid State Phenom. 162 (2010) 49–75.
[6] M. Kitano, M. Matsuoka, M. Ueshima, M. Anpo, Appl. Catal. A: Gen. 325 (2007) 1–14.
[7] M. Pelaez, N.T. Nolan, S.C. Pillai, M.K. Seery, P. Falaras, A.G. Kontos, P.S.M. Dunlop, J.W.J. Hamilton, J.A. Byrne, K. O'Shea, M.H. Entezari, D.D. Dionysiou, Appl. Catal. B: Environ. 125 (2012) 331–349.
[8] N. Serpone, J. Phys. Chem. B 110 (2006) 24287–24293.
[9] M. Mrowetz, W. Bakerski, A.J. Colussi, M.R. Hoffmann, J. Phys. Chem. B 108 (2004) 17269–17273.
[10] J.A. Rengifo-Herrera, K. Pierzchala, A. Sienkiwicz, L. Forro, J. Kiwi, C. Pulgarin, Appl. Catal. B: Environ. 88 (2009) 398–406.
[11] C.A. Emilio, M.I. Litter, M. Kunst, M. Bouchard, C. Colbeau-Justin, Langmuir 22 (2006) 3606–3613.
[12] V. Iliev, D. Tomova, L. Bilyarska, A. Eliyas, L. Petrov, Appl. Catal. B: Environ. 63 (2006) 266–271.
[13] R.J. Wilbraham, C. Boxall, R.J. Taylor, J. Photochem. Photobiol. A: Chem. 249 (2012) 21–28.
[14] T. Okuhara, N. Mizuno, M. Misono, Adv. Catal. 41 (1996) 113–252.
[15] L.R. Pizzio, P.G. Vázquez, C.V. Cáceres, M.N. Blanco, Appl. Catal. A: Gen. 256 (2003) 125–129.
[16] E. Papaconstantinou, Chem. Soc. Rev. 18 (1989) 1–31.
[17] A. Mylonas, E. Papaconstantinou, J. Mol. Catal. A: Chem. 92 (1994) 261–267.
[18] M. Blanco, L. Pizzio, Appl. Catal. A: Gen. 405 (2011) 69–78.
[19] P. Ngaotrakanwiwat, S. Saitoh, Y. Ohko, T. Tatsuma, A. Fujishima, J. Electrochem. Soc 150 (2003) A1405–A1407.
[20] G. Marc, E.I. García-López, L. Palmisano, Appl. Catal. A: Gen. 421/422 (2012) 70–78.
[21] J.A. Rengifo-Herrera, M.N. Blanco, L.R. Pizzio, Appl. Catal. B: Environ. 110 (2011) 126–132.
[22] C. Yu, J.C. Yu, W. Zhou, K. Yang, Catal. Lett. 140 (2010) 172–183.
[23] Y. Yang, Q. Wu, Y. Guo, C. Hu, E. Wang, J. Mol. Catal. A: Chem. 225 (2005) 203–212.
[24] K. Li, X. Yang, Y. Guo, F. Ma, H. Li, L. Chen, Y. Guo, Appl. Catal. B: Environ. 99 (2010) 364–375.
[25] N. Lu, Y. Zhao, H. Liu, Y. Guo, X. Yuan, H. Xu, H. Peng, H. Qin, J. Hazard. Mater. 199/200 (2012) 1–8.
[26] I. Holclajtner-Antunovic, D. Bajuk-Bogdanovic, M. Todorovic, U.B. Mioc, J. Zakrzewska, S. Uskokovic-Markovic, Can. J. Chem. 86 (2008) 996–1004.

[27] L.R. Pizzio, C.V. Cáceres, M.N. Blanco, Appl. Catal. A: Gen. 167 (1998) 283–294.
[28] J.T. Yates, Surf. Sci. 603 (2009) 1605–1612.
[29] V.M. Fuchs, E.L. Soto, M.N. Blanco, L.R. Pizzio, J. Colloid Interf. Sci. 327 (2008) 403–411.
[30] M. Pelaez, P. Falaras, V. Likadimos, A.G. Kontos, A.A. De la Cruz, K. O'shea, D. Dyonysiou, Appl. Catal. B: Environ. 99 (2010) 378–387.
[31] G.R. Hearne, J. Zhao, A.M. Dawe, V. Pischedda, M. Mazza, M.K. Nieuwoudt, P. Kibasomba, O. Memraoui, J.D. Comins, Phys. Rev. B 70 (2004) 134102-1–134102-10.
[32] I. Holclajtner-Antunovic, D. Bajuk-Bogdanovic, A. Popa, U.B.S. Uskokovic-Markovic, Inorg. Chim. Acta 383 (2012) 26–32.
[33] I. Holclajtner-Antunovic, U.B. Mioc, M. Todorovic, Z. Jovanovic, M. Davidovic, D. Bajuk-Bogdanovic, Z. Lausevic, Mater. Res. Bull. 45 (2010) 1679–1684.
[34] L. Li, Q.-Y. Wu, Y.-H. Guo, C.-W. Hu, Mater. Res. Soc. 87 (2005) 1–9.
[35] G. Colon, M.C. Hidalgo, J.A. Navio, A. Kubacka, M. Fernndez-García, Appl. Catal. B: Environ. 90 (2009) 633–641.
[36] A.L. Bassi, D. Cattaneo, V. Russo, C.E. Bottani, E. Barborini, T. Mazza, P. Piseri, P. Milani, F.O. Ernst, K. Wegner, S.E. Pratsinis, J. Appl. Phys. 98 (2005) 074305-1–074305-9.
[37] J.C. Parker, R.W. Siegel, Appl. Phys. Lett. 57 (1990) 943–945.
[38] M.T. Pope, Heteropoly and Isopoly Oxometalates, Springer-Verlag, Heidelberg, 1983p. p58.
[39] I.V. Kozhevnikov, Chem. Rev. 98 (1998) 171–198.
[40] R. Contant, Can. J. Chem. 65 (1987) 568–573.
[41] D. Carriazo, M. Addamo, G. Marcì, L. Palmisano, V. Rives, Appl. Catal. A: Gen. 356 (2009) 172–179.
[42] M. Pope, A. Muller, Angew. Chem. Int. Ed. Engl. 30 (1991) 34–48.
[43] R. Sivakumar, J. Thomas, M. Yoon, J. Photochem. Photobiol. C: Rev. 13 (2012) 277–298.
[44] T. Tachikawa, S. Tojo, M. Fujitsutka, T. Majima, Chem. Eur. J. 12 (2006) 3124–3131.
[45] D.T. Sawyer, Acc. Chem. Res. 14 (1981) 393–400.